

HEMOENCEPHALOGRAPHY TRAINING – AN EFFECTIVE METHOD FOR IMPROVING BRAIN FUNCTION PART 2. THE USE OF A COMPUTER APPLICATION SLORETA PARAMETER TO ANALYZE BRAIN WAVES AFTER HEMOENCEPHALOGRAPHY TRAINING

ANDRZEJ BARTOSIŃSKI¹, WANDA STANKIEWICZ¹,
KRYSTYNA ZIENIUK², MAŁGORZATA KIELCZEWSKA¹

¹ *Laboratory of Psychoneuroimmunology, Department of Microwave Protection
Military Institute of Hygiene and Epidemiology, Warsaw, Poland*

² *Military Institute of Medicine, Warsaw, Poland*

E-mail: andrzej.bartosinski@wihe.pl

Abstract: Hemoencephalography training is an effective method of improving the brain. It is a relatively cheap and easy method to use. This method was evaluated using standard encephalography (EEG) and the sLORETA software. The study involved a group of 70 volunteers. The change in spectral entropy in selected areas of the brain and the relative signal strength of the basic brain wave ranges were assessed.

Key words: neurofeedback, sLORETA, EEG, HEG, relative power, spectral entropy

DOI: 10.34668/PJAS.2018.4.4.01

Introduction

Electroencephalography (EEG) is the most important diagnostic method which uses electrical signals generated by the brain. EEG reflects the resultant electrical activity of the brain (and in particular the cerebral cortex) at a given moment. This activity is related to all processes in which the brain is involved. New technological advancements in the field of integrated electronics have led to the development of more precise caps and electrodes and thus, provides better quality signals generated by the brain.

EEG Analysis

For the analysis of the EEG signal sLORETA application (standardized Low Resolution Brain Electromagnetic Tomography) was used. The mapping of the charge distribution in the brain based on knowledge of tensions on the head of is a classic inverse problem. This task often occurs in various branches of science, where some parameters of the model must be determined based on the observed values [1]. In the study, the EEG analysis was used to evaluate the effects of hemoencephalography training (HEG).

Material and methods

Data were obtained from 70 healthy volunteers (men), aged from 18 to 36 years with a mean age of 26. None

of the respondents had been treated neurologically and/or psychiatrically in the past. Participants in the experiment were volunteers found through ads. All subjects were compensated for their participation in these experiments. The authors obtained the agreement of the Bioethics Committee of the Military Institute of Aviation Medicine (Decision No. 11/2016 06.22.2016) for research with the participation of volunteers. The test was carried out under laboratory conditions. Signals were recorded from 19 channels (assembly 10-20) from different regions on the head and from reference electrodes (ear) A1 and A2. Recording of the signal from the EEG electrodes was carried out during the pre-test (Before), biofeedback training (bfHEG) and post- biofeedback training (After). The test equipment used was NeXus-10 and NeXus-32 Fig. 1 (manufactured by the Dutch company MindMedia) [2]. An analog-to-digital converter was installed in the NeXus devices with 24-bit resolution on all sensors. EEG data were recorded using a 32-channel NeXus 32 recorder, equipped with active electrodes and 24-bit analog-to-digital converters. Standard caps with 19 electrodes and reference electrodes A1 and A2 were used for the test in accordance with the international system 10-20 (FP1, FP2, F7, F3, Fz, F4, F8, T3, T5, T4, T6, P3, Pz, P4, C3, Cz, C4, O1, O2, A1 and A2) [3]. The electrodes were placed according to the extended 10-20 system. For analysis of the EEG signals, the Biotrace package from MindMedia and sLORETA were used. The EEG system had a sampling

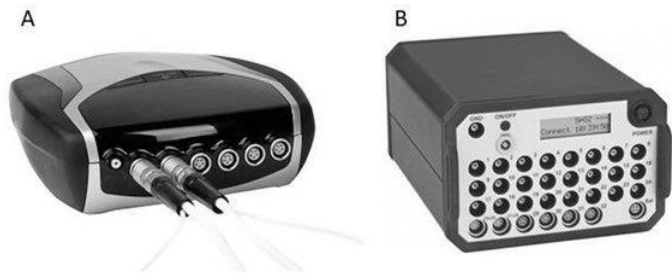


Fig. 1: Devices for multimodal registration: NeXus-10 (A) and NeXus-32 (B) (view of panels for connecting the sensors) [2].

frequency of 512 Hz. The HEG signal was determined using a head band (Fig. 2) and the blood volume pulse using a finger sensor. The registration of this signals took place at a sampling rate of 32 Hz.

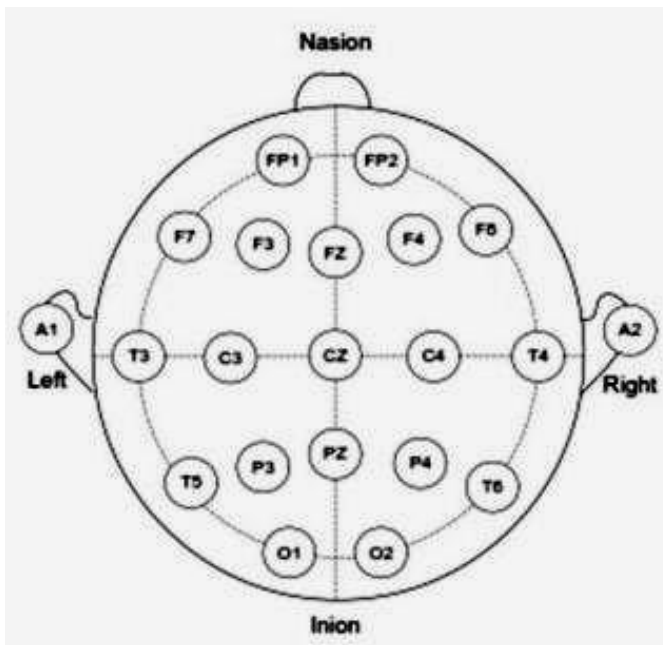


Fig. 3: International standard 10-20 position system of electrodes on human head [3].

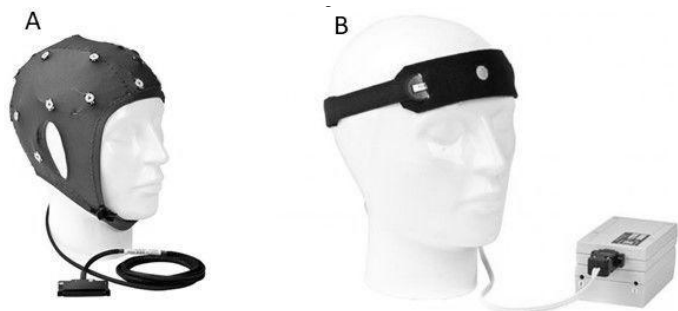


Fig. 2: EEG cap (19 channels, 2 reference electrodes and ground) [2] (A) and HEG device (manufactured by Biocomp reaserch Institute [4] (B)).

Table 1: Examples of electrode coordinates.

| Electrode | x | y | z |
|-----------|------------------|-----------|-----------|
| Fp1 | -32,81065 | 81,00142 | -3,699663 |
| Fp2 | 3281065 | 81,00142 | -3,699663 |
| C3 | -61,11541 | -13,06309 | 69,47281 |
| Cz | 0,00000001490116 | -10,31269 | 96,5361 |
| C4 | 61,11541 | -13,06309 | 69,47281 |

sLORETA software

Analysis using the sLORETA software requires an initial software configuration. The LORETA electrode creator renders a file with coordinates derived from electrodes corresponding to the EEG data used in the analysis. For all LORETA modules, the number of electrodes, the number of time intervals in each EEG data file and the sampling frequency were determined. The electrodes in the coordinate wizard were arranged in accordance with the international system 10-20 (Fig. 3). Table 1 presents the coordinates of the example electrodes.

Fig 3. shows the 10-20 system of electrode placement, where the letters A, C, F, O, P and T denote auricle, frontal, occipital, parietal and temporal regions, respectively. Odd and even numbering are used for the left and right sides, respectively. Midline electrodes are numbered with Z, representing zero. Nowadays, it is common to extend this 10-20 system by placing electrodes in between thus arriving at 32, 64, 128 and even 256 channels.

Sources are mapped in the Talairach space. The images comprise rectangular sections of the brain, from left to right, horizontal, sagittal and coronal views of the brain.

The x coordinates are negative for the left hemisphere and positive for the right hemisphere. The y coordinates are positive for the front and negative for the back locations. The coordinates are positive for the higher and negative for the near coaxial location.

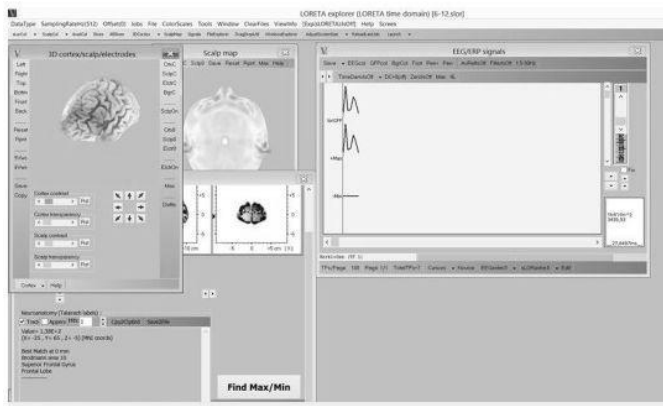


Fig. 4: Screenshot of software sLORETA.

LORETA employs statistical procedures for both types of data used in neuroimaging methods: ERP (time domain) and EEG (frequency domain) [1, 5, 6]. Current knowledge about the functions located in specific areas, frequency specifications, functional integration and the relationship between networks in the brain is still very limited. In recent years it has begun to be more evident that the location theory also does not fully allow the comprehensive understanding of brain functioning and the complexity of interaction between nerve connections. Typically, two approaches are used to analyze the pathways of brain activation for specific tasks. The first approach of distributing systems investigates correlations between physiological components. The second detects focal differences on the basis of a functionally specialized approach. Statistical tests used in the LORETA program are based on statistical mapping of parameters (statistical parameter SPM mapping). This approach uses the general linear model settings and creates a matrix for neurophysiological data. Specific effects (noise or specific activation) are estimated using the standard method of least squares or parameters of the estimated linear model such as differences in assessments determined each time by a specific effect. For each contrast, the statistic t (t - statistic) for each voxel (see Part I) is calculated to create a statistical map. Images are mapped to a standardized coordinate space, taking into account differences in the size and position of the brain, smaller images are averaged to amplify the signal in relation to noise. LORETA introduces similar SPM procedures with additional randomization and permutation tests. The tests are performed with a reference area obtained from all possible values of the statistical test for the observed points. Randomization and permutation tests are shown to check significance for the probability of false rejection of at least one family-wise error rate (FWER) in testing multiple hypotheses.

The functional mapping data analysis is usually performed on the basis of the voxels database by creating image statistics based on the differences between the conditions or the parameter map statistics. This procedure is created and takes into account simultaneous testing with the assumption of all voxels in the anatomical hypothesis. It should be noted that adequate neuroanatomical and neurophysiological knowledge is essential for the establishment of hypotheses in relation to the expected changes during the presentation of the experimental stimulus. LORETA contains a significant number of tools that allow the user to effectively monitor changes in EEG and LORETA sources within and between groups in an individual subject. It is important for reporting the results of therapy in neurofeedback training. Generally, neurofeedback training use computer-based conversion of EEG patterns to images on a computer screen. The person subjected to neurofeedback training le-

arns to influence these images and thus the self-regulation of the EEG (and what you are doing is self-regulation of the complex, dynamically changing nervous system).

Signal analysis

Spectral analysis is widely used to detect abnormalities in the EEG spectrum. Spectral entropy (SpecEn) measures the flatness of the signal spectrum and is considered a convenient way to analyze individual brain wave ranges. sLORETA software was used to calculate the spectral entropy changes and changes in relative signal power density relative density (RP) of the following brain wave ranges: delta, theta, alpha, beta and gamma.

The spectral analysis theoretically belongs to linear methods and transforms time series into a frequency domain. The methods used in the spectral analysis are fast Fourier Transform (FFT) and autoregression. Autoregression is more accurate, but FFT is simpler to use. Fourier transformation of the continuous time signal (Continuous Time Fourier Transform, CTFT):

$$X(\omega) = F(x(t)) = \int_{-\infty}^{\infty} x(t)e^{-j\omega t} dt \quad (1)$$

where $\omega = \frac{2\pi}{T} = 2\pi f$, f is the frequency in Hz. As a result of this transformation, the continuous signal in the time domain $x(t)$ is converted into the continuous signal $X(\omega)$ in the frequency domain. In signal analysis, we usually deal with discrete samples of the signal $x(nT_s)$ or simply $x(n)$, where T_s is the sampling period. This transformation is called Discrete Time Fourier Transform (DTFT):

$$X(\omega) = \sum_{n=-\infty}^{\infty} x(nT_s)e^{-j\omega nT} \quad (2)$$

It should be remembered that in both cases the function and signal must meet certain conditions that ensure the feasibility of transformation. Both transformations are reversible i.e. you can reconstruct the original signal based on them. These dependencies are defined by the formulas [7]:

$$x(t) = F^{-1}(X(\omega)) = \frac{1}{2\pi} \int_{-\infty}^{\infty} X(\omega)e^{j\omega t} d\omega \quad (3a)$$

$$x(nT_s) = F^{-1}(X(\omega)) = \frac{T_s}{2\pi} \int_{-\pi/T_s}^{\pi/T_s} X(\omega)e^{j\omega nT_s} d\omega \quad (3b)$$

The spectral power (the function of the power spectral density) of continuous and discrete signals is calculated as the Fourier transform of the autocorrelation function (these equations are called Wiener- Chinczyn equations) [8]:

$$P_{xx}(f) = \int_{-\infty}^{\infty} R_{xx}(\tau)e^{-j2\pi f t} d\tau \quad (4a)$$

$$P_{xx}(f) = \sum_{m=-\infty}^{\infty} R_{xx}(m) e^{-j2\pi f m / f_{pr}} \quad (4b)$$

where $f_{pr} = \frac{1}{T_s}$ is the sampling frequency, τ is the continuous signal shift, and m displacement of the discrete signal. The correlation functions are defined as follows:

$$R_{xx}(\tau) = E[x(t)x(t-\tau)] \quad (5a)$$

$$R_{xx}(m) = E[x(n)x(n-m)] \quad (5b)$$

where $E[\cdot]$ is the expected value. Another way to estimate the signal's power spectrum is to calculate it directly using the Fourier transform (without determining the correlation) [9]:

$$S_{xx} = \frac{|X(f)|^2}{N} \quad (5)$$

Spectral entropy (Power Spectral Entropy) was introduced in 1992 by J.N. Kapur. Procedure for calculating the spectral entropy of a random variable $X = x_1, x_2, \dots, x_n$ for $n \geq 1$ and corresponding probabilities of events $P = \{p_1, p_2, \dots, p_n\}$ $0 \leq p_i \leq 1, i = 1, 2, \dots, n$ $\sum_{i=1}^n p_i = 1$ [10, 11] is as follows:

- calculation of discrete Fourier transform (DTFT) $X(\omega_i)$, where ω_i is i -th frequency,
- calculation of normalized power spectral density (PSD_n):

$$PSD_n(\omega_i) = \frac{1}{N} |X(\omega_i)|^2 \quad (6)$$

- calculation of the distribution function of normalized power density:

$$p_i = \frac{PSD_n(\omega_i)}{\sum_{i=1}^n PSD_n(\omega_i)} \quad (7)$$

- the last step is the calculation of entropy:

$$SpecEn = - \sum_{i=1}^n p_i \ln p_i \quad (8)$$

In addition, the relative signal power density was computed for a selected range for each frequency theta, alpha, beta and gamma rays by the equation:

$$RP = \frac{\sum_{i=j}^{i=k} PSD_n(\omega_i)}{\sum_i^n PSD_n(\omega_i)} \quad (9)$$

where j and k determine the frequency ranges of an individual brain wave. The fraction numerator contains the normalized power density of the selected frequency range (appropriate for a given brain wave), and the denominator contains the total normalized signal density covering all frequency ranges of the analyzed brain waves (from $i = 0.5$ Hz to $n = 64$ Hz).

Results

Analysis of the variability of the EEG signal may be used to quantify the level of perfusion in selected parts of the brain. These signals have been grouped in 5 regions corresponding to areas on the surface of the head and cortex. Spectral Entropy (SpecEn) for low and high frequencies reflects the slowdown in brain electrical activity in subjects who have not yet “activated” the cerebral circulation within the frontal lobes as a result of biofeedback training. The results relating to the preliminary examination were marked as “Before” in the figures and the results after the biofeedback training as “After”. Spectrum entropy increased in all regions studied. The relative signal strength increased in the case of alpha and beta waves in all regions (Fig. 8 and 9) and decreased in the case of theta wave in all regions (Fig. 7). In the case of delta and gamma waves, the increase or decrease in the relative signal strength depended on the region of the brain (Fig. 6 and 10).

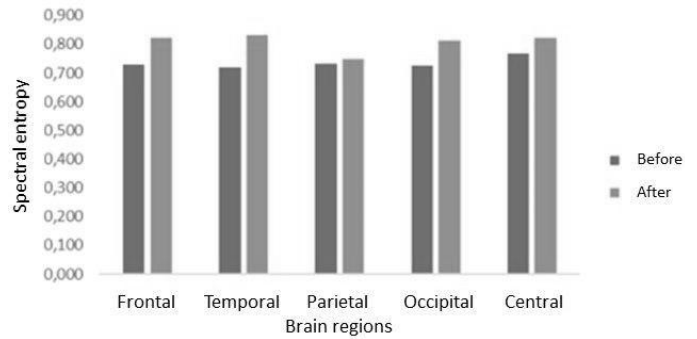


Fig. 5: Changes in spectral entropy calculated using the sLORETA software of the EEG signal recorded before and after biofeedback (bfHEG).

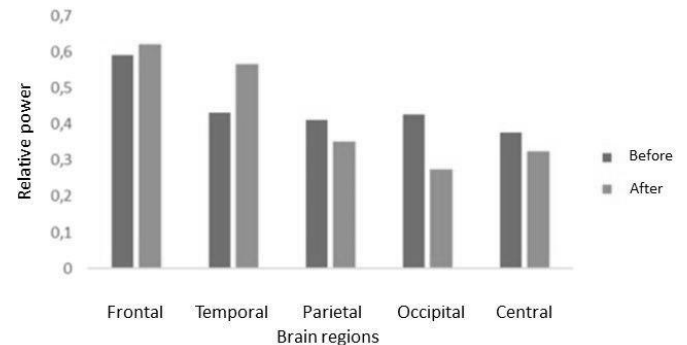


Fig. 6: Changes in relative delta wave power obtained from the EEG signal recorded before and after biofeedback (bfHEG) calculated using the sLORETA software.

Fig. 12 – 14 provide a graphic illustration of changes in the activity of beta waves in selected areas of the brain (identified by spatial coordinates, Brodmann area number, and name of the anatomical structure) and associated brain

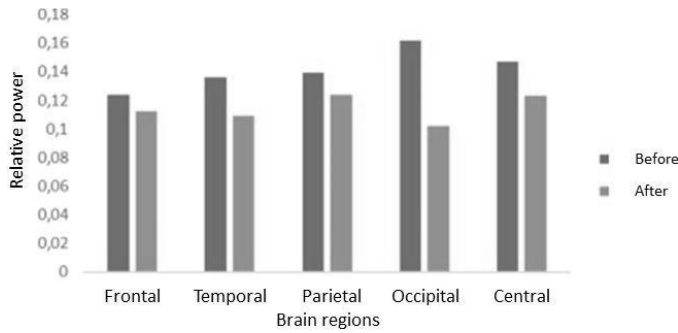


Fig. 7: Changes in relative theta wave power obtained from the EEG signal recorded before and after biofeedback (bfHEG) calculated using the sLORETA software.

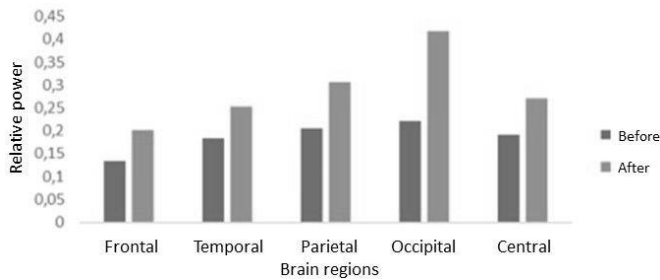


Fig. 8: Changes in relative alpha wave power obtained from the EEG signal recorded before and after biofeedback (bfHEG) calculated using the sLORETA software.

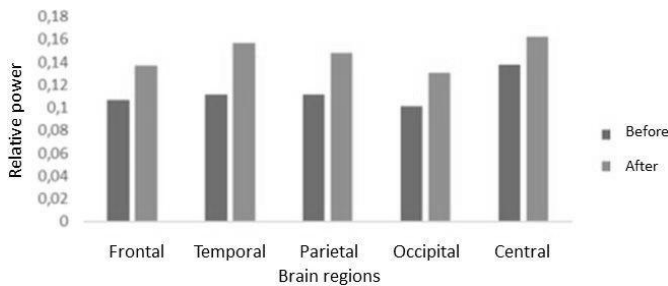


Fig. 9: Changes in relative beta wave power obtained from the EEG signal recorded before and after biofeedback (bfHEG) calculated using the sLORETA software.

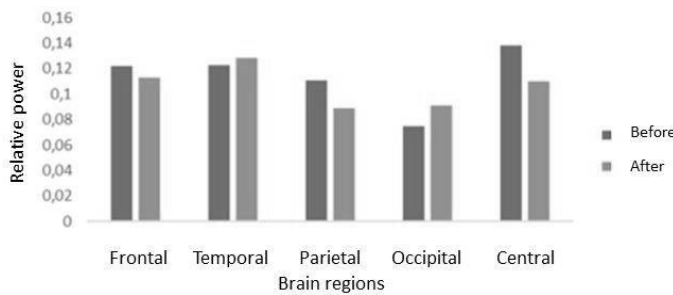


Fig. 10: Changes in relative gamma wave power obtained from the EEG signal recorded before and after biofeedback (bfHEG) calculated using the sLORETA software.

wave activities depicted as the intensity of the shading of a given area.

In Fig. 11 A maximum value: (X= 32, Y= 45, Z= 29), Brodmann area 10, Anterior prefrontal cortex (most rostral part of superior and middle frontal gyri), and minimum values: (X= 25, Y= -39, Z= 1), Brodmann area 4, Primary Motor Cortex (It is located in the posterior portion of the frontal lobe) [12]. In Fig. 11 B maximum Values: (X= 53, Y= 10, Z= 1), Brodmann area 22, Superior Temporal Gyrus, and minimum values: (X= 4, Y= -39, Z= 71), Brodmann area 4, Primary Motor Cortex.

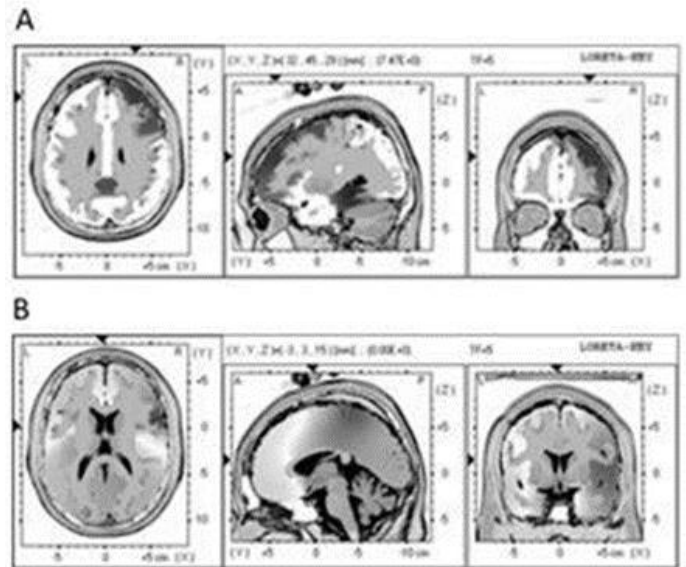


Fig. 11: The distribution of electrical charge density in the brain estimated by the solution of the inverse problem (sLORETA) applied to the 21-channel EEG recording before (A) and after (B) hemoencephalography training – SMR (beta wave).

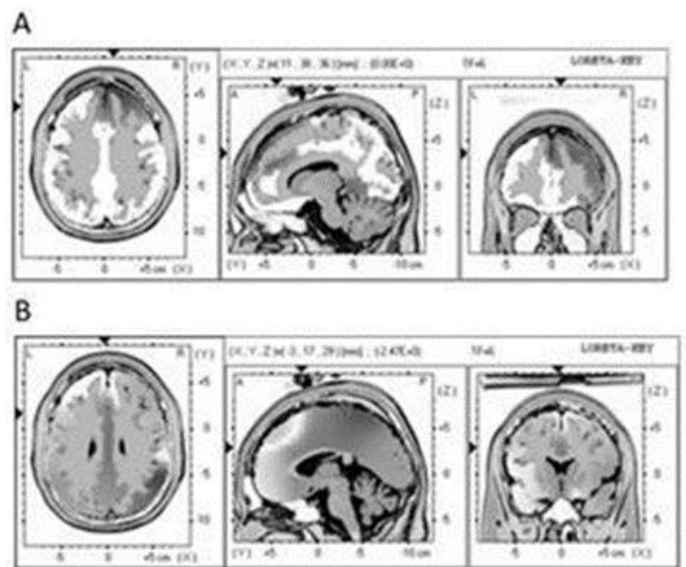


Fig. 12: The distribution of electrical charge density in the brain estimated by the solution of the inverse problem (sLORETA) applied to the 21-channel EEG recording before (A) and after (B) hemoencephalography training – beta 1 wave.

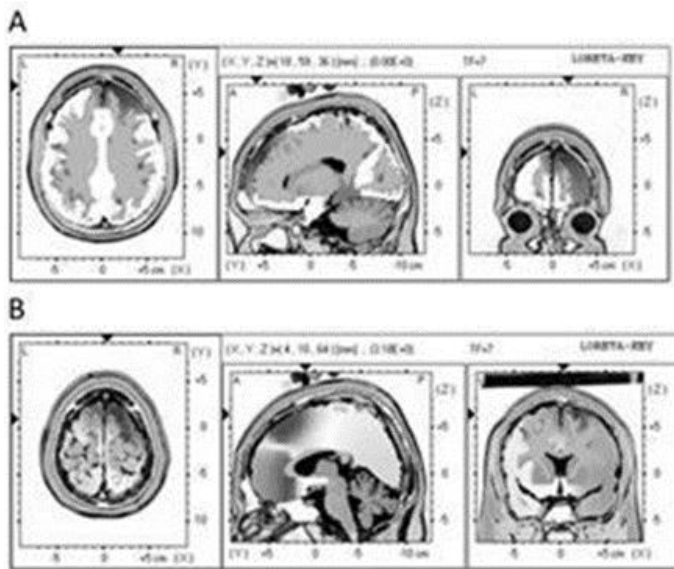


Fig. 13: The distribution of electrical charge density in the brain estimated by the solution of the inverse problem (sLORETA) applied to the 21-channel EEG recording **before** (A) and **after** (B) hemoencephalography training – beta 2 wave.

In Fig. 12 A maximum value: ($X = 11, Y = 59, Z = 36$), Brodmann area 9, Dorsolateral prefrontal cortex, and minimum values: ($X = -31, Y = -39, Z = -20$), Brodmann area 20, Inferior temporal gyrus. In Fig. 12 B maximum values: ($X = 60, Y = -4, Z = 8$), Brodmann area 22, Superior Temporal Gyrus, and minimum values: ($X = 32, Y = -53, Z = 64$), Brodmann area 7, Visuo-Motor Coordination.

In Fig. 13 maximum value: ($X = 11, Y = 59, Z = 36$), Brodmann area 9, Dorsolateral prefrontal cortex, and minimum values: ($X = -24, Y = -39, Z = -13$), Brodmann area 36, Ectorhinal area, now part of the perirhinal cortex (in the rhinal sulcus). In Fig. 13 B maximum values: ($X = 18, Y = 10, Z = 64$), Brodmann area 6, Premotor cortex and Supplementary Motor Cortex (Secondary Motor Cortex) (Supplementary motor area), and minimum values: ($X = -3, Y = 31, Z = -6$), Brodmann area 32, Dorsal anterior cingulate cortex.

Conclusions

Biofeedback training resulted in an increase in the alpha and theta waves activity, while the delta wave activity decreased. Such changes in brain waves activity are positive since they are accompanied by a decrease in beta 3 activity (with the increase of beta 1 and beta 2 activity) which is the most energy-intensive range of the brain (due to the high amplitude of this signal).

The research was partly financed from the grant No. DOBR/0038/R/ID2/2013/03.

Literature

- [1] Pascual-Marqui R.D. Standardized low-resolution brain electromagnetic tomography (sloreta): technical details. *Methods Find Exp Clin Pharmacol*, 24(Suppl D):5–12, 2002.
- [2] User manual for the biotrace+ software nexus-16 & nexus-32 ©mind media b.v., 2004-2006.
- [3] Palaniappan R. *Biological signal analysis*. BookBoon, 2011.
- [4] <https://www.biocompresearch.org/heg-neurofeedback>, 2018.
- [5] Pascual-Marqui R. et al. Functional imaging with low resolution brain electromagnetic tomography (loreta): review, new comparisons, and new validation. *Japanese Journal of Clinical Neurophysiology*, 30:81–94, 2002.
- [6] Pascual-Marqui R.D. et al. Functional imaging with low-resolution brain electromagnetic tomography (loreta): a review. *Methods and findings in experimental and clinical pharmacology*, 24(Suppl C):91–95, 2002.
- [7] Osowski S. Cyfrowe przetwarzanie sygnałów z zastosowaniem matlaba. *Oficyna Wydawnicza Politechniki Warszawskiej*, 2016.
- [8] Zieliński T.P. *Cyfrowe przetwarzanie sygnałów: od teorii do zastosowań*. Wydawnictwa Komunikacji i Łączności, 2007.
- [9] Osowski St., Cichocki A., Siwek K. *Matlab w zastosowaniach do obliczeń obwodowych i przetwarzania sygnałów*. Oficyna Wydawnicza Politechniki Warszawskiej, Warszawa, 2006.
- [10] Ellerkmann R.K. et al. Spectral entropy and bispectral index as measures of the electroencephalographic effects of sevoflurane. *Anesthesiology: The Journal of the American Society of Anesthesiologists*, 101(6):1275–1282, 2004.
- [11] Zhang A., Yang B., Huang L. Feature extraction of eeg signals using power spectral entropy. In *BioMedical Engineering and Informatics. BMEI 2008. International Conference on. 2008. IEEE*, 2008.
- [12] Baars B.J., Gage N.M. *Cognition, brain, and consciousness: Introduction to cognitive neuroscience*. Academic Press, 2010.

Received: 2018

Accepted: 2018